Science Advances
AAAS

Supplementary Materials for

The strength of surgical knots involves a critical interplay between friction and elastoplasticity

Paul Johanns *et al.*

Corresponding author: Pedro M. Reis, pedro.reis@epfl.ch

Sci. Adv. **9**, eadg8861 (2023)
DOI: 10.1126/sciadv.adg8861

The PDF file includes:

Other Supplementary Material for this manuscript includes the following:

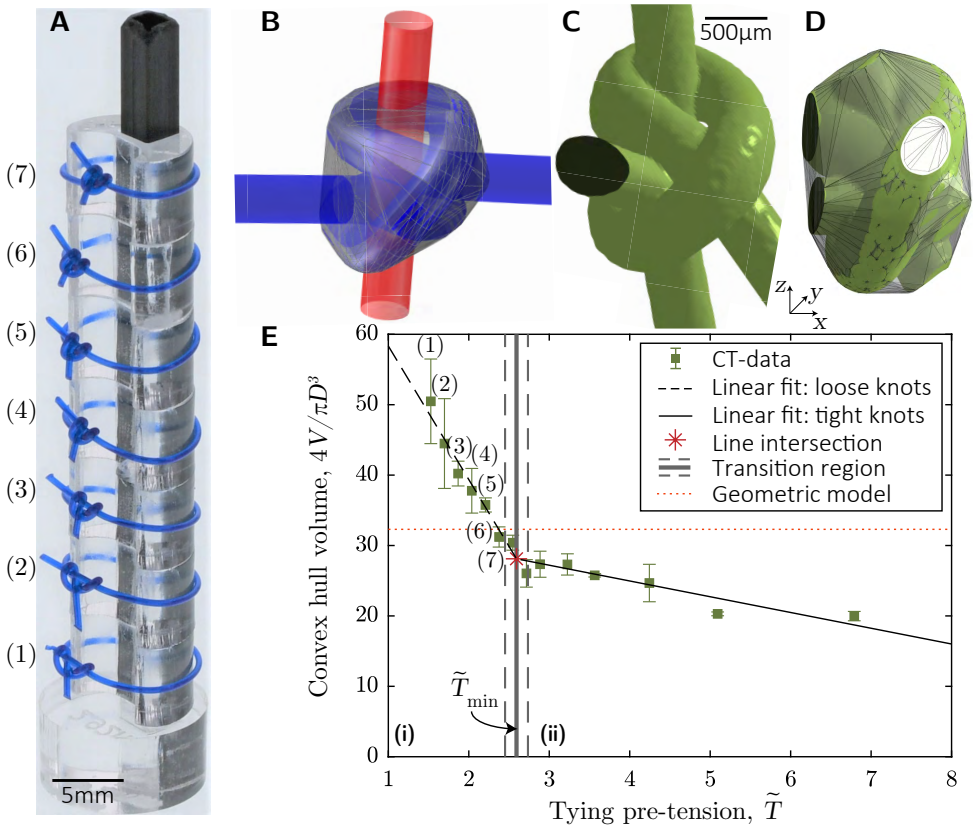

Fig. S1: Definition of the onset of tight knots. (**A**) Photograph of 7 sliding granny knots of different tightness (increasing from bottom to top) mounted on holders, for μCT scanning. (**B**) Tightest ideal S || S knot configuration *(34)*. A convex hull (transparent grey surface) is applied to the bulk knot, excluding the protruding strands. (**C**) 3D reconstructed S || S knot (7) with its four protruding strands. (**D**) Bulk S || S knot after the protruding strands were removed by image processing. A convex hull (transparent grey surface) is applied on the resulting volume. (**E**) Normalized convex-hull volume, $4V/\pi D^3$, as a function of the applied tying pre-tension, $\tilde{T}$. The experimental data (symbols) exhibits two distinct slopes, which are described by linear fittings of seven consecutive data points; the first fit (dashed, black line) for low pre-tensions and the second one (continuous black line) for high pre-tensions. The intersection point is obtained from the intersection of the fitted lines, yielding the transition region, $\tilde{T}_{\text{min}} = 2.59 \pm 0.14$ (vertical line). The volume of the convex hull applied on the tightest, ideal S || S knot is represented by the dotted horizontal line.

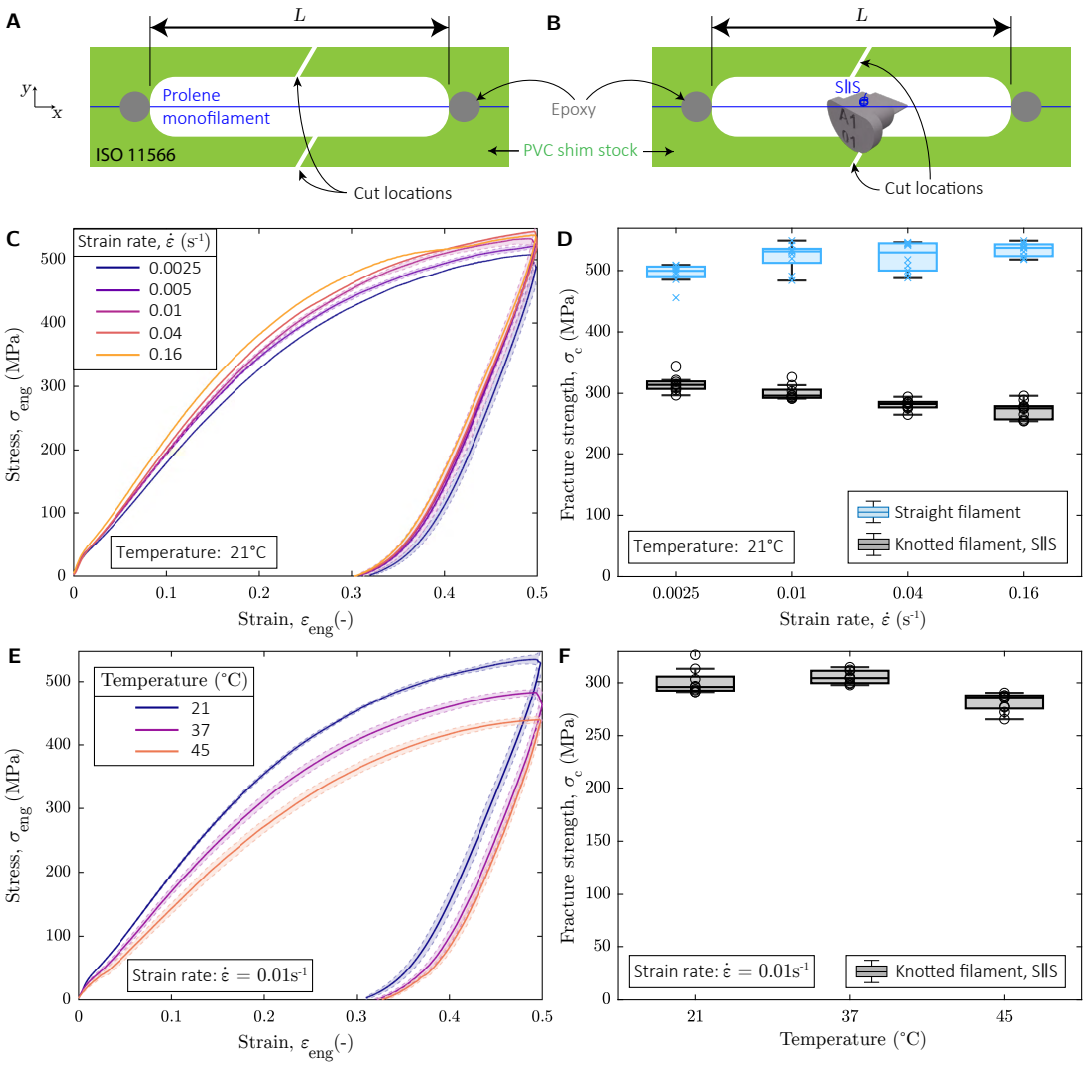

Fig. S2: Rate- and temperature-dependence of the monofilaments. (**A**) Schematic of a straight, un-knotted Prolene (3-0 USP) monofilament glued with epoxy on a frame of Polyvinyl chloride (PVC) shim stock, setting the gauge length, L (following Ref. *(43)*). (**B**) The same testing technique as in **A**, with the addition of a S || S knot tied on a rigid pin. (**C**) Rate-dependence on the engineering stress-strain behavior of straight filaments, recorded at room temperature (21°C). (**D**) Rate-dependence on the fracture strength, σ_c, of straight and knotted (S || S) filaments, at room temperature (21°C). (**E**) Temperature-dependence on the engineering stress-strain response of straight filaments, measured at a strain rate, $\dot{\varepsilon} = 0.01/\text{s}$. (**F**) Temperature-dependence on the fracture strength, σ_c, of knotted (S || S) filaments, at the strain rate $\dot{\varepsilon} = 0.01/\text{s}$.

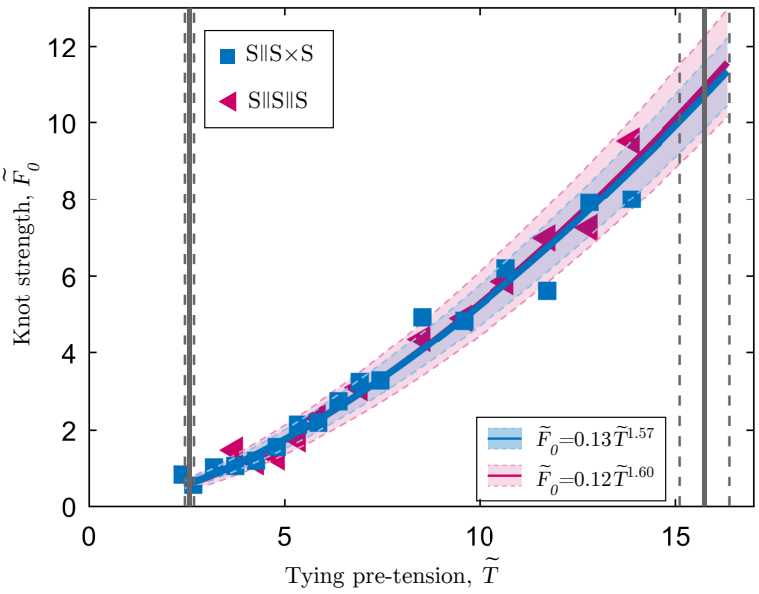

Fig. S3: Equivalence of knot topology. Knot strength, $\tilde{F}_0$ as a function of applied tying pre-tension, $\tilde{T}$, for the S || S×S and the S || S || S knot. Eq. (1) of the main text is used to fit both data sets (see legeng).

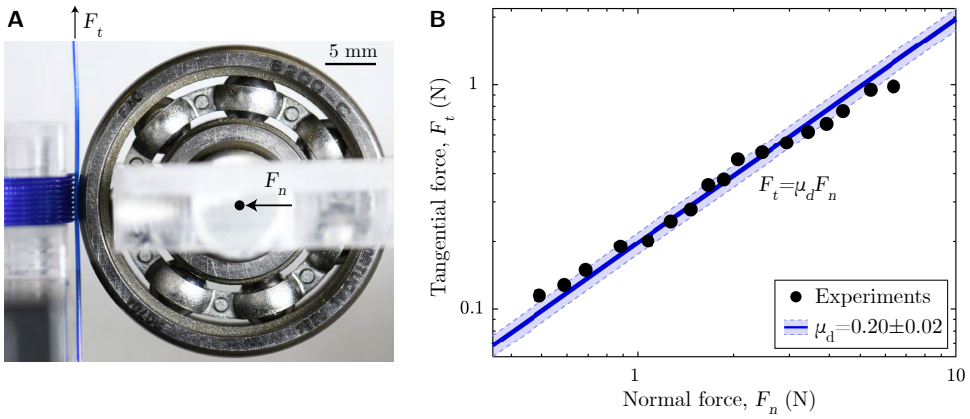

Fig. S4: Characterization of the kinematic friction coefficient between Prolene monofilaments. (**A**) Photograph of the setup consisting of a vertical straight filament, which is pressed by a ball bearing with the force F_n against a layer of coiled monofilaments. (**B**) Tangential force measurements, F_t, as a function of imposed normal force, F_n. The solid line and shaded region represent the linear fit and the corresponding confidence interval.

		n	Configuration	μ	α	$\widetilde{K}$	$\beta_1=\widetilde{K}/n$	$\beta_2=\widetilde{K}/n\mu$
Experiments	◀	2	S‖S	0.2	1.62	0.07	0.036	0.18
	■	3	S‖S×S	0.2	1.57	0.13	0.043	0.21
	▶	3	S×S×S	0.2	1.60	0.12	0.041	0.20
	♦	4	S‖S×S×S	0.2	1.59	0.16	0.040	0.20
	●	5	S‖S×S×S×S	0.2	1.56	0.21	0.041	0.21
	▲	6	S‖S×S×S×S×S	0.2	1.63	0.24	0.040	0.20
Mean:					1.59		0.040	0.20
Standard deviation:					0.03		0.002	0.01

Table S1: Summary of parameters.

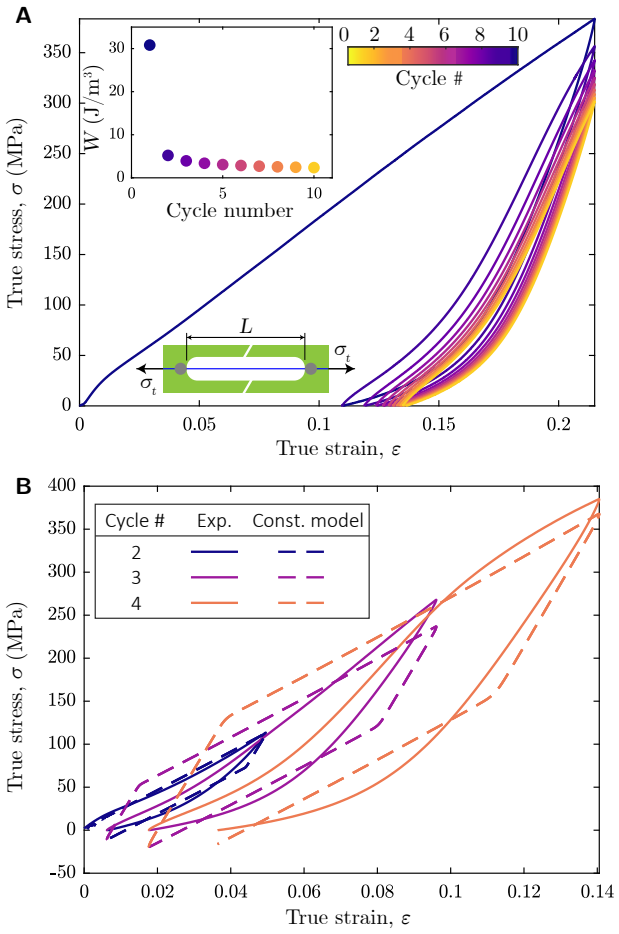

Fig. S5: Plasticity modeling of surgical filaments. (**A**) True stress, σ, as a function of true strain, ε, of Prolene 1 in a cyclic, uniaxial-tension test, for 10 cycles. The schematic in the lower inset illustrates the specimen preparation. The plot in the upper inset quantifies the dissipated energy density, W, between 10 consecutive cycles. (**B**) Cyclic tensile response of a pre-stretched filament with increasing maximum strain, plotted as true stress, σ, versus true strain, ε. Our constitutive model for elastic-viscoplastic mechanical behavior is fit onto the experimental data.

Parameters:	E (MPa)	σ_0 (MPa)	σ_{Sat} (MPa)	h (MPa)
Initial guess	6000	5	50	2
Lower bound	5000	0.1	30	0.5
Upper bound	7000	30	450	20
Fitted param.	5060.9	1.25	137.5	0.5

$\rightarrow G$=1687.0 MPa

Table S2: Calibration of material parameters using experimental data.

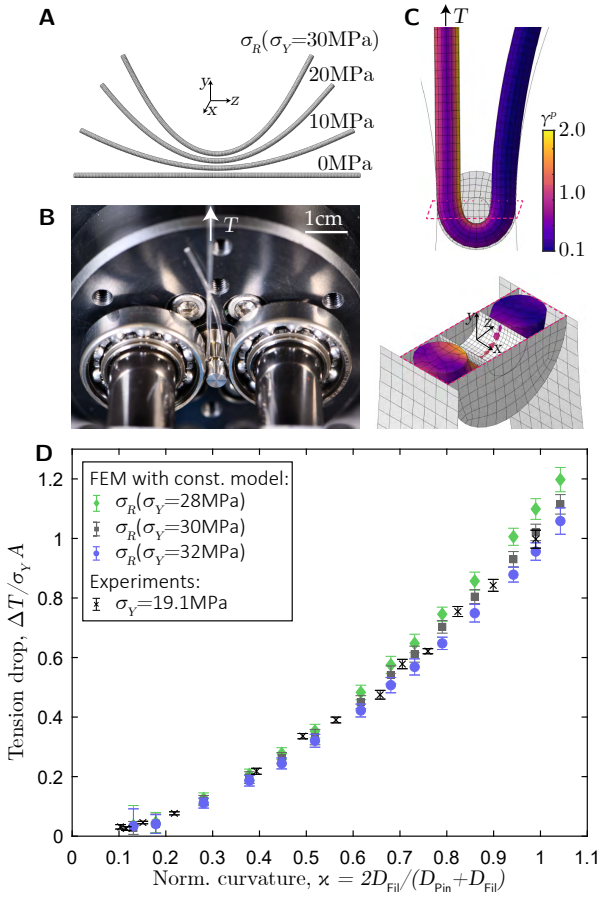

Fig. S6: Calibration of plasticity model in bending. (**A**) Snapshots, obtained from the FEM simulations, of the deformed shape of the originally-straight filament, before ($\sigma_R = 0$) and after it has been subjected to residual bending stresses, $\sigma_R(\sigma_Y)$, with $\sigma_Y = \{10, 20, 30\}$ MPa. (**B**) Photograph of the plastic capstan apparatus used to quantify plastic dissipation by measuring the tension drop, ΔT, across the two ends. (**C**) FEM snapshot of the plastic capstan system, visualizing equivalent plastic shear strain, γ^p in a side view and in the horizontal cutting plane (purple dashed line). (**D**) Dimensionless tension drop, $\Delta T/(\sigma_Y A)$, as a function of normalized curvature, $\kappa = 2D_{\text{Fil}}/(D_{\text{Pin}} + D_{\text{Fil}})$. The elasto-plastic material model is calibrated by tuning the residual stresses, with the fitting parameter to $\sigma_Y = 30 \pm 2$ MPa, in order to match the experimental data (see legend).

MOVIE CAPTIONS

Movie S1: Knot-tying procedure by a surgeon. An experienced surgeon manually ties the S || S×S knot (number of throws, $n = 3$) in a Prolene polypropylene filament (3-0 USP) on a rigid support. The surgeon was asked to tighten the knots identically to their routine suturing procedures.

Movie S2: Illustration of an analog physical model of wound dehiscence failure. Three stitches of different levels of tightness (S || S×S each) were tied on a suturing practice pad, which was fabricated in-house using silicone-based vinyl polysiloxane, VPS32 (Elite Double 32, Zhermack) with two colored layers (each 2 mm in thickness). For visualization purposes, the knots were tied in two different monofilament materials of the same diameter, 3-0 USP; Prolene polypropylene filament in blue and Ethilon nylon suture in black. The outer knots, k_1 and k_3, are initially tighter than the middle knot, k_2. To emulate, for illustration purposes, the typical surgical failure mode of wound dehiscence, the pad was loaded by gradually increasing the magnitude of the far-field uniaxial stress field, σ_∞. At a sufficiently large stress level, the filament of the middle knot, k_2, starts sliding until it completely slips out and, therefore, no longer fulfills its binding function.

Movie S3: S || S knot tied in purely elastic rods. The surgical sliding knots investigated in this study, tied in *elasto-plastic* Prolene monofilaments, do not unravel, even in the case of vanishing friction coefficients. This movie highlights the importance of plastic deformation of slippery filaments by showcasing a case where the filaments are fully elastic (i.e., without plasticity). An S || S knot was tied in *purely elastic* filaments (vinyl polysiloxane, VPS32, Elite Double 32, Zhermack). Frictional interactions in the regions of self-contact of the knotted filament (dynamic friction coefficient $\mu = 0.35 \pm 0.02$) guarantee the knot topology. Then, silicone oil (viscosity: 1000 cSt) was applied and distributed on the filament surfaces to lubricate the contact regions, thereby reducing (likely deactivating) friction significantly. Consequently, in the absence of frictional forces, the stored elastic bending energy of the bent filament drives the unraveling of the knot.

Movie S4: Plastic capstan system. The apparatus of the *plastic capstan* configuration allowed us to calibrate the parameters of our plasticity model. Specifically, we quantified the tension drop, ΔT, between the free and pulled ends of a monofilament (1 USP) passing through a grooved pin. Here, the depicted pin is of diameter, $D_{\text{Pin}} = 1$ mm, and mounted on a central rotary air-bearing. The two laterally constraining ball bearings (left and right) are nearly frictionless and in contact with the outer surface of the pin. Consequently, the dissipation during the displacement-controlled pulling process (speed of 1 mm/s) is only due to plastic bending deformation of the filament wrapping the pin, causing the tension to drop between the two extremities.

Movie S5: Knot tying, tightening & testing in the FEM simulations. Using the FEM software package ABAQUS/EXPLICIT (Simulia, Dassault Systèmes), an S || S knot was tied using two of unit diameter, $D_{\text{Fil}} = 1$ filaments. The filaments were initially straight. The numerical tying procedure involved the following series of steps. In Step I, a residual stress field was applied on filament (2) before the S || S knot was tied around filament (1), which was subject to an axial dead load Mg. In Step II, the ends of filament (1) were aligned orthogonally with filament (2), and the two rigid stopper plates compacted the knot. Next, the extremities of filament (1) were gradually loaded by the tying pre-tension of the same magnitude, $\tilde{T}$, but in

opposing directions. Before the testing procedure, the pre-tensions were released while the knot was uni-laterally freed from a stopper plate. Finally, the sliding filament (1) was displaced with constant unit speed, pulling the S || S knot against the remaining rigid stopper plate, allowing the measurement of the slipping force, $\tilde{F}$. During the complete animation, the equivalent plastic shear strain, γ^p, is visualized on the filaments (see colorbar in the movie).

Data S1: the raw data used to generate each of the plots in the figures of both the Main Text and Supplementary Information. Each sheet within the file is dedicated to a particular figure, with column headings denoting the plotted quantities, as indicated in the captions of the corresponding figures. For figures featuring multiple panels, the pertinent data is consolidated within the same sheet.